ISSN 1070-4280, Russian Journal of Organic Chemistry, 2019, Vol. 55, No. 12, pp. 1864–1868. © Pleiades Publishing, Ltd., 2019.
Russian Text © The Author(s), 2019, published in Zhurnal Organicheskoi Khimii, 2019, Vol. 55, No. 12, pp. 1870–1876.

New Reaction of Dimethylformamide with Acrylic Acid

A. G. Akhmadullina[a],* R. M. Akhmadullin[a], A. S. Gazizov[b], A. T. Gubaidullin[b], and A. V. Lisin[c]

[a] *"AhmadullinS Science and Technologies" Research and Development Center, Kazan, 420029, Russia*

[b] *Arbuzov Institute of Organic and Physical Chemistry, Kazan Scientific Center, Russian Academy of Sciences, Kazan, 420088 Russia*

[c] *Kazan National Research Technological University, Kazan, 420015 Russia*

**e-mail: ahmadullins@gmail.com*

Received May 28, 2019; revised October 18, 2019; accepted October 24, 2019

Abstract—A new homogeneous reaction of dimethylformamide (DMF) with acrylic acid was studied. The reaction afforded previously unknown 3-[2-carboxyethyl(dimethyl)azaniumyl]propanoate and carbon monoxide. The product structure was determined by ^{1}H and ^{13}C NMR spectroscopy, X-ray diffraction, and elemental analysis, and evolution of gaseous carbon monoxide was confirmed by GC/MS. The kinetic parameters of the described reaction and its overall order were determined.

Keywords: *N*,*N*-dimethylformamide, acrylic acid, inner salt, quaternary ammonium base, reaction kinetics.

DOI: S107042801912008X

Tetraalkylammonium salts containing a carboxy group are known due to their surfactant [1], bactericidal, and antimicrobial properties [2, 3], and they can be used to obtain hydrophilic coatings [4] and stabilize various nanoparticles [5, 6]. Synthetic approaches to such compounds are based on reactions of halogen-substituted carboxylic acids with tertiary amines [7], of alkyl halides with acids containing a tertiary amino group [8], and of lactones with tertiary amines [9]. Also, the addition of tertiary amines to acrylic acid (aza-Michael reaction) has been reported [10]. On the other hand, there are no published data on reactions of dimethylformamide (DMF, **1**) with unsaturated carboxylic acids with the formation of quaternary ammonium bases.

Herein, we report the liquid-phase reaction of DMF (**1**) with acrylic acid (**2**). The product of this reaction was previously unknown inner salt, 3-[2-carboxyethyl-(dimethyl)azaniumyl]propanoate (**3**). It was formed from 1 equiv of **1** and 2 equiv of **2** with liberation of 1 equiv of carbon monoxide (**4**) according to Scheme 1. Presumably, the first stage of this reaction is thermal decarbonylation of **1** to give dimethylamine which adds to acrylic acid (**2**) to produce 3-(*N*,*N*-dimethylamino)-propanoic acid; the subsequent addition of the second acrylic acid molecule yields final product **3**.

Compound **3** is a white crystalline powder melting at 146–148°C and is readily soluble in water. The evolution of gaseous carbon monoxide (**4**) was detected by GC/MS; the mass spectrum contained the base peak with *m*/*z* 28 $[CO]^+$ and two low-intense peaks with *m*/*z* 16 $[O]^+$ and 12 $[C]^+$. The structure of **3** was confirmed by ^{1}H and ^{13}C NMR spectra (see Experimental) and finally proved by X-ray analysis. Compound **3** crystallized in the *Cc* space group belonging to the monoclinic crystal system and had zwitterionic structure. The asymmetric part of its unit cell contained one independent molecule (Fig. 1). It should be noted that molecule **3** possesses its own C_{2v} symmetry; therefore, its structure can be erroneously solved as the one be-

Scheme 1.

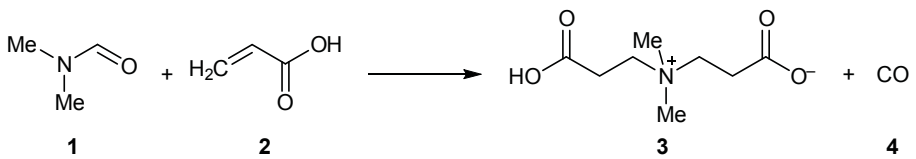

1 **2** **3** **4**

Table 1. Parameters of intermolecular hydrogen bonds in the crystal structure of **3** according to the X-ray diffraction data

D–H···A	D–H, Å	H···A, Å	D···A, Å	∠DHA, deg	Symmetry operation
O^3–H^3···O^2	0.94(6)	1.50(6)	2.436(5)	175(5)	–1/2 + *x*, 5/2 – *y*, –1/2 + *z*
C^1–H^{13}···$O^{3'''}$	0.96	2.36	3.298(6)	167	*x*, –1 + *y*, *z*
C^2–H^{23}···$O^{2'''}$	0.96	2.38	3.323(6)	167	*x*, –1 + *y*, *z*
C^1–H^{11}···$O^{2'}$	0.96	2.33	3.262(6)	163	–1/2 + *x*, –1/2 + *y*, *z*
C^2–H^{21}···O^{3*}	0.96	2.34	3.265(6)	162	1/2 + *x*, –1/2 + *y*, *z*
C^1–H^{12}···$O^{4''}$	0.96	2.49	3.178(6)	129	*x*, 1 – *y*, 1/2 + *z*
C^2–H^{22}···O^{1**}	0.96	2.51	3.203(6)	129	*x*, 1 – *y*, –1/2 + *z*

longing to a higher-symmetry space group (C_2/c) since extinction analysis of the initial reflection set indicated the existence of pseudo-symmetry elements; however, in this case, the asymmetric part of a unit cell of **3** would contain only a half of its molecule. Our choice of space group was based not only on the best refinement convergence but also on the fact that the given molecule cannot be placed in a particular position since one of the carboxy groups is deprotonated. It was found that the length of one of the four N–C bonds in molecule **3** appreciably differs from the three others and that the C^8–O^3 bond length allows it to be reliably identified.

The supramolecular structure of compound **3** in crystal is formed as a result of both classical O–H···O intermolecular hydrogen bonds and weaker C–H···O contacts (Table 1). The basic motif, zigzag chains of H-bonded molecules along the *a*0*c* axis (Fig. 2), involves hydrogen bonding between the O^2 and H^3 atoms. The O^3 and O^2 oxygens simultaneously participate in classical and bifurcated C–H···O hydrogen bonds (Table 1) with the H^{13} and H^{23} methyl hydrogen atoms of the neighboring molecule which is related to the initial molecule by translation along the 0*b* axis. As a result, H-bonded molecular chains form a two-dimensional structure represented by layers parallel to the [–101] crystallographic plane (Fig. 3). This fairly tight packing mode is stabilized by additional C–H···O hydrogen bonds between the layers, so that the calculated packing factor is 73.2%; this value approaches the upper limit of the range typical of organic crystals (65–75%), and the unit cell lacks voids potentially accessible for solvent molecules.

The kinetics of the homogeneous liquid-phase reaction of **1** with **2** were studied by the differential method. The reaction in excess DMF (**1**) was found to be of 2nd order in acrylic acid (**2**) at its different initial concentrations (Fig. 4a). The kinetic curves were plotted by measuring the change of the CO pressure in the reactor. The slope of the log dependence of the initial reaction rate on the initial acrylic acid concentration is equal to 1.98 (Fig. 4b). Compound **3** crystallized from the mixture on cooling.

Likewise, first order of the reaction with respect to DMF in excess acrylic acid was determined (Fig. 5a).

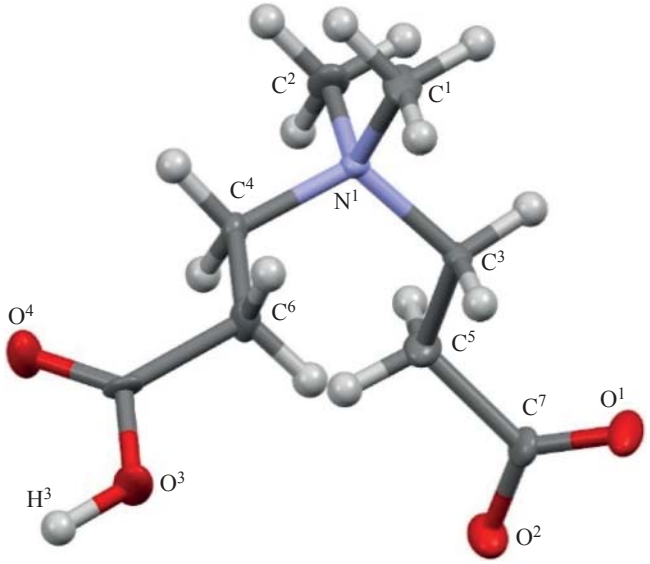

Fig. 1. Structure of the molecule of 3-[2-carboxyethyl-(dimethyl)azaniumyl]propanoate (**3**) in crystal according to the X-ray diffraction data with partial atom numbering. Non-hydrogen atoms are shown as thermal vibration ellipsoids with a probability of 50%; hydrogen atoms are shown as arbitrary sized spheres. Selected bond lengths: O^1–C^7 1.215(5), O^2–C^7 1.274(6), O^3–C^8 1.313(5), O^4–C^8 1.233(6), N^1–C^1 1.510(7), N^1–C^3 1.515(5), N^1–C^4 1.512(5), N^1–C^2 1.489(7) Å.

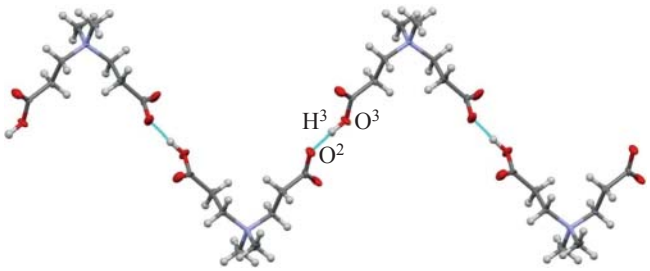

Fig. 2. Zigzag chains formed by molecules **3** in crystal through classical hydrogen bonds O–H···O.

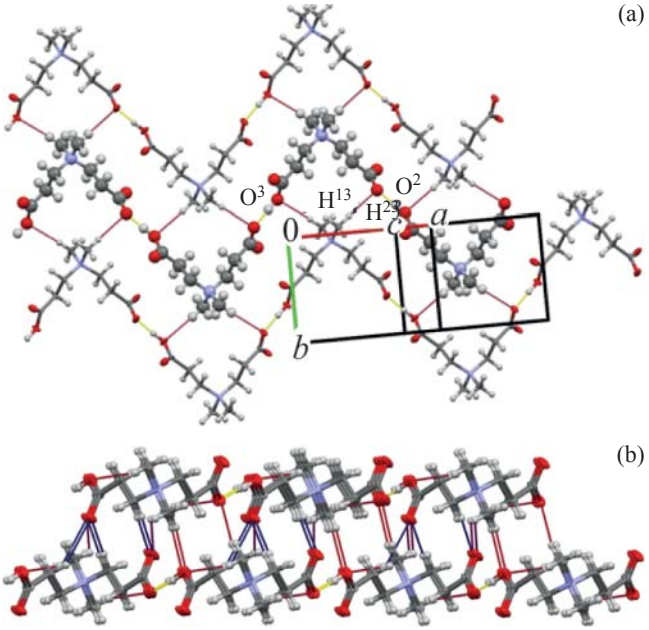

Fig. 3. Intermolecular O–H···O (yellow) and C–H···O interactions (red, blue) in the crystal structure of **3**; views along the (a) [–101] crystallographic plane and (b) 0*b* crystallographic axis.

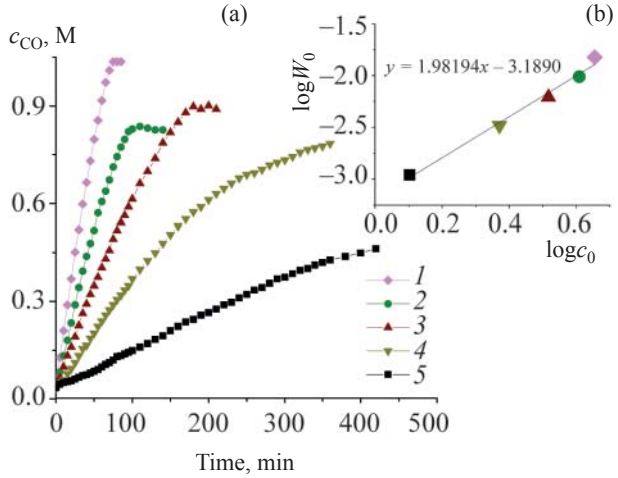

Fig. 4. (a) Kinetic curves for the evolution of carbon monoxide at different initial concentrations of acrylic acid (**2**); (b) log dependence of the initial reaction rate on the initial acrylic acid concentration; DMF (**1**), 1.29 mol; acrylic acid (**2**), mol: (*1*) 0.69, (*2*) 0.56 mol, (*3*) 0.42, (*4*) 0.28, (*5*) 0.14; temperature 180°C.

The slope of the log dependence of the initial reaction rate on the initial DMF concentration is equal to 0.74 (Fig. 5b). In this case, final product **3** did not crystallize from excess acrylic acid (**2**) on cooling.

The overall order of the reaction is 3, and the kinetic equation is as follows:

$$v = kc_1c_2^2,$$

where v is the reaction rate, k is the rate constant, and c_1 and c_2 are the concentrations of DMF (**1**) and acrylic acid (**2**), respectively.

Figure 6a shows the kinetic curves at a stoichiometric reactant ratio at different temperatures. The rate constants were calculated from the 3rd-order kinetic equation:

$$K = \frac{1}{2t}\cdot\left(\frac{1}{c^2}-\frac{1}{c_0^2}\right),\ \text{L}^2\ \text{mol}^{-2}\ \text{s}^{-2}.$$

The energy of activation and pre-exponential factor were determined from the plot of $\ln k$ versus $1000/T$ (Fig. 6b). The slope of this plot is equal to E_a/R, and the intercept on the y axis corresponds to $\ln A$ (E_a is the energy of activation, R is the universal gas constant equal to 8.3144 J mol^{-1} K^{-1}, and A is the pre-exponential factor). The energy of activation calculated by the Arrhenius equation for the temperature range 150–180°C and reactant concentrations c_1 = 0.278 M and c_2 = 0.555 M was 102.05 kJ/mol, and the pre-exponential factor was estimated at 6.2×10^7 L^2 mol^{-2} s^{-2}. We thus obtained the following equation for the calculation of the reaction rate:

$$v = 6.2\times10^7\exp(102050/RT)c_1c_2^2.$$

In summary, we were the first to describe the reaction of dimethylformamide (**1**) with acrylic acid (**2**), which led to the formation of quaternary ammonium base **3**. Zwitterionic compound **3** was formed in one step with a high yield.

EXPERIMENTAL

The ^{1}H and ^{13}C NMR spectra were recorded on a Bruker Avance 600 spectrometer (Germany) at 400 and 100.6 MHz, respectively; the ^{1}H chemical shifts were measured relative to the residual proton signal of the solvent (D_2O).

The X-ray analysis of a 0.26×0.39×0.68-mm single crystal of **3** was performed at the Diffraction Methods Laboratory, Federal Joint Spectral Analytical Center, Arbuzov Institute of Physical and Organic Chemistry (Kazan Scientific Center, Russian Academy of Sciences). The data were acquired at 23°C using a Bruker Kappa Apex II CCD automated X-ray diffractometer (Germany) (Mo K_α radiation, λ 0.71073 Å, graphite monochromator, ω/2θ scanning, $-20 \le h \le 18$, $-10 \le k \le 10$, $-18 \le l \le 18$, $3.52° \le \theta \le 36.95°$). Total of 4716 reflection intensities were measured, including 3227 independent reflections (R_{int} = 0.0332)

and 2641 reflections with $I \geq 2\sigma(I)$. Monoclinic crystal system, space group *Cc*; $C_8H_{15}NO_4$, *M* 189.21; unit cell parameters (23°C): *a* = 12.5996(8), *b* = 6.5432(4), *c* = 11.1421(7) Å; β = 97.923(3)°; *V* = 909.8(1) Å^3; *Z* = 4; d_{calc} = 1.381 g/cm^3. The data were collected and edited, and the unit cell parameters were refined, using APEX2 [11]. A correction for absorption (μ_{Mo} = 0.110 mm^{-1}) was applied using SADABS [12]. The structure was solved by the direct method and was refined by the least squares method first in isotropic and then in anisotropic approximation (for all non-hydrogen atoms) using SHELXL [13]. The coordinates of hydrogen atoms were determined from the difference electron density maps and were refined according to the riding model. Final divergence factors: R = 0.0432, R_w = 0.1036 for 3227 reflections with $F^2 = 2\sigma$ and R = 0.0558, R_w = 0.1125 foe all independent reflections; goodness of fit 1.031; number of variables 122; maximum and minimum electron density peaks 0.397 and –0.210 *e* Å^{-3}, respectively. All calculations were performed on a PC using WinGX [14]. Intermolecular interactions were analyzed, and molecular structures were plotted using PLATON [15] and Mercury [16]. The coordinates of atoms and other crystallographic parameters of compound **3** were deposited to the Cambridge Crystallographic Data Centre (CCDC entry no. 1914538) and are available at *http://www.ccdc.cam.ac.uk/data_request/cif* upon request.

The melting point of **3** was measured with a Buchi M-560 melting point apparatus (Switzerland). The liberated gas was analyzed on a Maestro-IL gas–liquid chromatograph (Russia) coupled with an Agilent 5975 mass-selective detector and equipped with Agilent GC/MSD ChemStation software. The elemental composition of **3** was determined with a Euro EA 3000 analyzer (Italy).

Commercial *N*,*N*-dimethylformamide (chemically pure grade, GOST 20289-74) and acrylic acid (CAS no. 79-10-7; Acros Organics) were used.

3-[2-Carboxyethyl(dimethyl)azaniumyl]propanoate (3). A 250-mL cylindrical stainless-steel high-pressure reactor equipped with a pressure gage, thermocouple, and Heildolph MR-Hei-Standard magnetic stirrer was charged with 94.4 g (1.292 mol) of DMF (**1**) and 10.0–50.0 g (0.139–0.694 mol) of acrylic acid (**2**) (excess DMF) or 100.0 g (1.388 mol) of **2** and 5.3–20.3 g (0.073–0.278 mol) of **1**. The reactor was heated at 150–190°C for 75 to 440 min, and the pressure therein increased up to 4.0 MPa. When finished, the stirrer and heater were turned off. When the mixture cooled down to 30°C, the pressure was released to atmospheric,

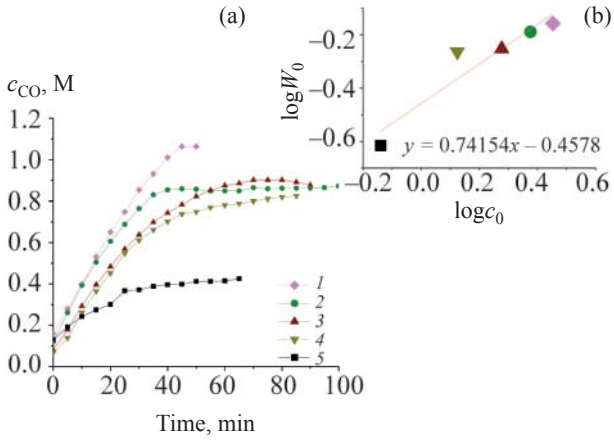

Fig. 5. (a) Kinetic curves for the evolution of carbon monoxide at different initial concentrations of DMF (**1**); (b) log dependence of the initial reaction rate on the initial DMF concentration; acrylic acid (**2**), 1.39 mol; DMF (**1**), mol: (*1*) 0.35, (*2*) 0.28 mol, (*3*) 0.21, (*4*) 0.14, (*5*) 0.074; temperature 180°C.

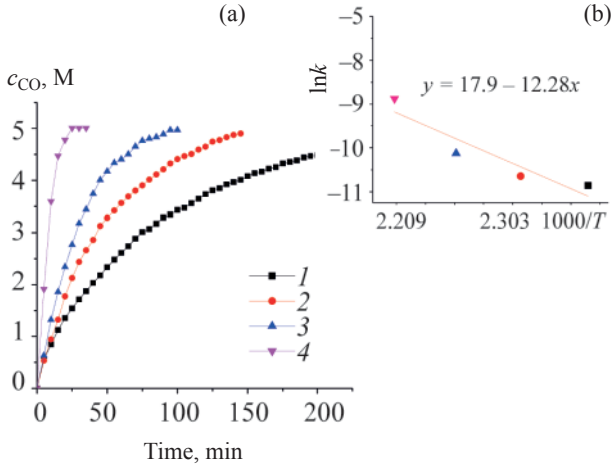

Fig. 6. (a) Kinetic curves for the evolution of carbon monoxide in the reaction of 0.278 mol of DMF (**1**) with 0.555 mol of acrylic acid (**2**) at (*1*) 150, (*2*) 160, (*3*) 170°C, and (*4*) 180°C and (b) Arrhenius plot for this reaction.

and the reactor was cooled to 10°C and opened. In the reaction with excess DMF, the precipitate of **3** was filtered off, washed with petroleum ether, and dried for 24 h at room temperature.

The reaction with 94.4 g (1.292 mol) of DMF and 52.5 g (0.729 mol) of acrylic acid at 170°C (2 h) gave 53.28 g (77.4%) of **3**. The pressure in the reactor increased to 4.5 MPa during the synthesis. The reaction of 20.3 g (0.278 mol) of DMF with 40.0 g (0.555 mol) of acrylic acid (stoichiometric reactant ratio) at 190°C in 10 min gave 47.3 g (92.0%) of **3**. ^{1}H NMR spectrum (D_2O), δ, ppm: 5.19–5.28 m (3-H), 5.48 m (4-H), 5.98–6.02 m (2-H), 7.24 s (1H, OH). ^{13}C NMR spectrum

(D_2O), δ_C, ppm: 29.19–30.11 (C^4), 50.35–50.42 (C^2), 60.44 (C^3), 174.86–175.97 (C^1). Found, %: C 55.92; H 7.99; N 7.09. $C_8H_{15}NO_4$. Calculated, %: C 57.78; H 7.99; N 7.40; O 33.82.

The CO pressure was recalculated to concentration using the ideal gas equation:

$$pV = nRT,$$

where p is the CO pressure (Pa), V is the gas volume (m^3), R is the universal gas constant (8.31 J K^{-1} mol^{-1}), T is the absolute temperature (K), and n is the number of moles of the gas.

CONFLICT OF INTERESTS

The authors declare the absence of conflict of interests.

REFERENCES

1. Chen, X., Xin, Y., Yu, F., and Lan, Z., *J. Surfactants Deterg*., 2017, vol. 20, p. 1121. https://doi.org/10.1007/s11743-017-1987-z
2. Chen, Sh., Chen, Sh., Jiang, S., Mo, Y., Tang, J., and Ge, Z., *Surf. Sci*., 2011, vol. 605, p. 25. https://doi.org/10.1016/j.susc.2011.03.013
3. Li, L., Zhao, Y., Zhou, H., Ning, A., Zhang, F., and Zhao (Kent), Z., *Tetrahedron Lett*., 2017, vol. 58, p. 321. https://doi.org/10.1016/j.tetlet.2016.12.021
4. Zhang, S., Yang, X., Tang, B., Yuan, L., Wang, K., Liu, X., Zhu, X., Li, J., Ge, Z., and Chen, S., *Chem. Eng. J*., 2018, vol. 336, p. 123. https://doi.org/10.1016/j.cej.2017.10.168
5. Cai, C., Li, X., Wang, Y., Liu, M., Shi, X., Xia, J., and Shen, M., *Chem. Eng. J*., 2019, vol. 362, p. 842. https://doi.org/10.1016/j.cej.2019.01.072
6. Zhao, G., Dong, X., and Sun, Y., *Langmuir*, 2019, vol. 35, p. 1846. doi 10.1021/acs.langmuir.8b01921
7. Hussain, S.M.Sh., Kamal, M.Sh., and Fogang, L.T., *J. Mol. Liq*., 2018, vol. 266, p. 43. https://doi.org/10.1016/j.molliq.2018.06.031
8. Zhen-Jie, M., Xuesong, D., Zhi-Yan, C., and Bao-Hang, H., *ACS Appl. Mater. Interfaces*, 2018, vol. 10, p. 41350. https://doi.org/10.1021/acsami.8b14671
9. Wang, M., Xiao, Y., Lin, L., Zhu, X., Du, L., and Shi, X., *Bioconjugate Chem*., 2018, vol. 29, p. 1081. https://doi.org/10.1021/acs.bioconjchem.7b00747
10. Rumyantsev, M.S., Kazantsev, O.A., Rumyantsev, S.A., and Kalagaev, I.Yu., *Comput. Theor. Chem*., 2018, vol. 1129, p. 16. https://doi.org/10.1016/j.comptc.2018.02.017
11. APEX2 (Version 2.1), SAINTPlus. Data Reduction and Correction Program (Version 7.31A), Bruker Advanced X-ray Solutions, Madison, Wisconsin: Bruker AXS, 2006.
12. Sheldrick, G.M., *SADABS, Program for Empirical X-ray Absorption Correction*, Delft: Bruker-Nonius, 2004.
13. Sheldrick, G.M., *SHELXTL, Structure Determination Software Suite, v. 6.1*, Madison, Wisconsin: Bruker AXS, 2000.
14. Farrugia, L.J., *J. Appl. Crystallogr*., 1999, vol. 32, p. 837. https://doi.org/10.1107/S0021889899006020
15. Spek, A.L., *J. Appl. Crystallogr*., 2003, vol. 36, p. 7. https://doi.org/10.1107/S0021889802022112
16. Macrae, C.F., Edgington, P.R., McCabe, P., Pidcock, E., Shields, G.P., Taylor, R., Towler, M., and van de Streek, J., *J. Appl. Crystallogr*., 2006, vol. 39, p. 453. https://doi.org/10.1107/S002188980600731X